Diffusion of Ag adatom on the H-terminated and clean Si(111) surfaces: A first-principles study

Hojin Jeong and Sukmin Jeong*
Department of Physics, Chonbuk National University, Chonju 561-756, Korea
(Received 8 March 2004; revised manuscript received 16 July 2004; published 11 January 2005)

Using a first-principles calculation method, we investigate the adsorption and diffusion of a Ag adatom on the H-terminated and clean Si(111) surface, which would be useful in understanding the initial stages of metal growth on semiconductor substrates. We perform extensive searches for metastable surface structures induced by the Ag adatom adsorption, and then find its diffusion barriers and pathways on both kinds of the substrates. The calculated barrier for the Ag atom on the H-terminated surface is only 0.14 eV. On the clean surface, the diffusion barriers inside a half–unit cell (HUC) and between HUC's are calculated at 0.27 and 0.88 eV, respectively. The present results provide a qualitative description of the Ag growth modes on the Si(111) surfaces: the three-dimensional island growth on the H-terminated surface and the formation of the wetting layer on the clean surface. In addition, the calculated barrier of 0.88 eV agrees well with the diffusion barrier measured by recent scanning-tunneling microscopy.

DOI: 10.1103/PhysRevB.71.035310 PACS number(s): 68.43.Jk, 68.43.Fg, 68.43.Bc, 68.47.Fg

I. INTRODUCTION

Heteroepitaxial growth of ultrathin metal films on semiconductor surfaces is a highly important issue in surface science and technology. To obtain high-quality metal films, it is essential to control the growth mode of the films, which is sensitive to the mobility of the adsorbate atoms and to the balance of free energies among the surfaces, interfaces, and overlayer films. Introduction of foreign atomic layers on the substrates, hence, alters both surface kinetics and energetics and consequently changes the growth mode of the films remarkably.[1–3]

Such drastic changes of the epitaxial growth of metal films are seen in comparing the metal films deposited on the H-terminated and clean Si(111) surfaces. When Ag is deposited onto the clean Si(111)7×7 surface, for instance, growth proceeds in a layer-by-layer fashion at room temperature (RT) and in a Stranski-Krastanov (SK) growth mode with $\sqrt{3}\times\sqrt{3}$ phase transition at 300 °C.[4–8] In contrast, the Ag growth mode on the H-terminated Si(111) surface changes the Volmer-Weber (VW) mode, in which three-dimensional Ag islands are formed.[2,9–11]

It is commonly argued that the mobility of the adsorbed metal adatoms is enhanced on the H-terminated Si(111) surface compared to that on the clean Si(111) surface.[4,12] Scanning-tunneling microscopy (STM) studies showed that the mobility of the metal adatoms between the half–unit cells (HUC's) of Si(111) 7×7 is much lower than that inside a HUC.[13–15] Recently, another STM study directly determined the Ag adatom barrier for inter-HUC diffusion at 0.93 eV.[16] However, the detailed processes for metal diffusion on the H-terminated and clean Si(111) surfaces are still unknown and, in order to find the origins for the different growth behaviors, comparative studies for both kinds of substrates are required.

In the present study, using a first-principles method, we investigate Ag adsorption and diffusion on the H-terminated and clean Si(111) surfaces, as a model system for metal diffusion, which can provide important information on the growth mode of metal on a semiconductor substrate. On the H-terminated Si(111) surface, the Ag adatom has an extremely small diffusion barrier of 0.14 eV. On the clean Si(111) surface, we find two distinct energy barriers for Ag diffusion inside a HUC and between HUC's with 0.27 and 0.88 eV. The calculated results are consistent with various growth behaviors of Ag on the Si(111) surfaces and quantitatively the barrier between HUC's, 0.88 eV, agrees well with the measured value, 0.93 eV.[16]

II. CALCULATION METHOD

All calculations have been performed by use of Vienna ab initio simulation package[17] (VASP), which incorporates ultrasoft pseudopotentials[18] and the spin-independent generalized-gradient approximation (GGA) of Predew and Wang[19] for the exchange-correlation energy. We employ repeated slab geometries, in which each slab is separated by a 10-Å-wide vacuum layer. The bottom of the slab has a bulk-like structure with each Si atom saturated by a H atom. The geometry optimization has been performed for all atoms except for the bottom-most H and Si atoms until the remaining force acting on each ion is less than 1.0×10^{-2} eV/Å. We use the 15-Ry cutoff energy for the plane wave basis. To establish the calculational accuracy, we perform extensive convergence tests with respect to the cutoff energy for bulk Si, bulk Ag, and a silane (SiH_4) molecule. Table I shows the calculated values of lattice constants (a), cohesive energies (E_c), and bulk moduli (B) for bulk Si and Ag, and the calculated Si-H bond length (l) and symmetric stretching vibration frequency (ν_s) for SiH_4. The lattice constants, cohesive energies, and Si-H bond length already converge at 15 Ry. The bulk moduli and vibration frequency obtained by the 15-Ry cutoff energy agree with the fully converged values obtained by the 30-Ry cutoff-energy with the differences of 1.2% and 1.6%, respectively.

The clean Si(111) 7×7 surface, upon H exposure, converts into the 1×1 structure. For the simulation on the H-terminated Si(111) surface, we use the 3×3 in-plane pe-

TABLE I. Calculated structural properties of bulk Si, bulk Ag, and a silane (SiH_4) molecule at different cutoff energies: For bulk Si and Ag, lattice constants (a), cohesive energies (E_c), and bulk moduli (B) and for SiH_4, Si-H bond length (l) and symmetric stretching vibration frequency (ν_s). Note that all calculations have been performed with respect to spin-unpolarized Si and Ag atoms.

Cutoff energy (Ry)		10	15	20	30	Expt.
Si	a(Å)	5.46	5.46	5.46	5.46	5.43[a]
	E_c(eV)	5.32	5.33	5.33	5.33	4.63[a]
	B(MBar)	0.86	0.86	0.87	0.87	0.99[a]
Ag	a(Å)	4.23	4.17	4.17	4.17	4.09[a]
	E_c(eV)	2.41	2.63	2.62	2.62	2.95[a]
	B(MBar)	0.81	0.86	0.88	0.87	1.01[a]
SiH_4	l(Å)	1.49	1.48	1.48	1.48	1.48[b]
	ν_s(cm^{-1})	2044	2064	2109	2097	2187[b]

[a]Ref. 36.
[b]Ref. 37.

riodic supercell with six Si layers and 2×2 k-point mesh for surface Brillouin zone (SBZ) sampling.[20] For the clean Si(111) surface, for calculational efficiency, we adopt two kinds of supercells: For the Ag diffusion inside a HUC, we use the 4×4 supercell with four Si adatoms and four Si rest atoms locally arranged in a 2×2 pattern, and for the inter-HUC diffusion, we take the 5×5 metastable structure[30] that contain dimer rows at the boundaries between HUC's. The detailed features of the surface structures will be described later. The 4×4 supercell contains six Si layers and a 2×2 k-point mesh is used for SBZ sampling. The Si(111) 5×5 surface is built thicker (eight Si layers) than the 4×4 surface to consider the missing corner holes. We take one k point at the Γ point in SBZ for this surface.

The convergence test is also performed with respect to k-point sampling. In increasing the k-point mesh to 4×4 from 2×2 in the 3×3 and 4×4 supercells, and to 2×2 from the Γ point in the 5×5 cell, the relative total energies of the metastable structures of a Ag adatom do not change within 0.03, 0.01, and 0.01 eV, respectively. This means that the present k-point samplings for the three different supercells are sufficient for reliable results.

III. RESULTS

A. Ag on the H/Si(111) surface

In order to obtain the diffusion barrier for the Ag adatom on the H/Si(111) surface, we first calculate the potential energy surface (PES) as a function of the in-plane position of the Ag adatom (Fig. 1). For the Ag adatom on the H/Si(111) surface, the substitutional adsorption, where the adatom makes direct bonds with the substrate with breaking of a H-substrate bond,[3] does not take place. Furthermore, the substrate structures do not change significantly upon Ag adsorption. Thus the in-plane position of the adatom is a good parameter for describing the surface diffusion of a Ag adatom.

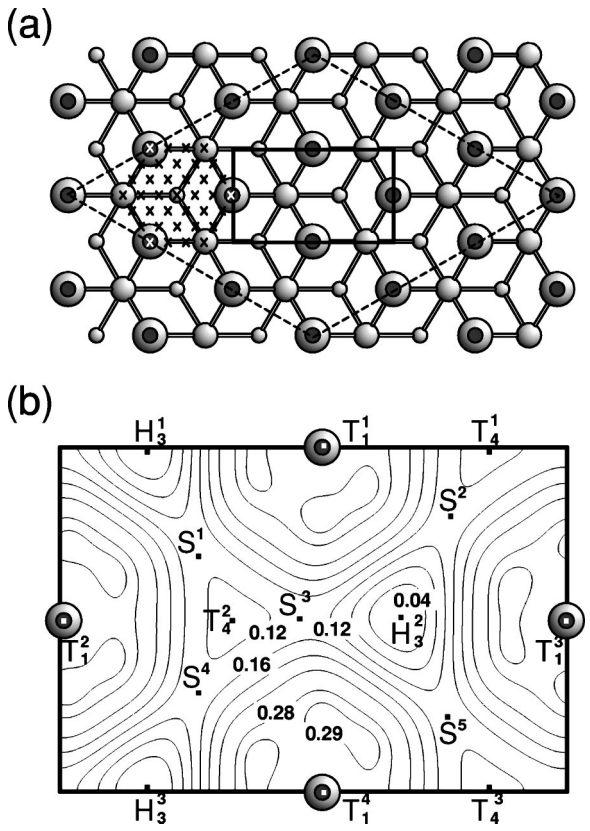

FIG. 1. (a) Top view of the H-terminated Si(111) 1×1 surface, where white and black spheres represent Si and H atoms, respectively. The dashed parallelogram indicates the 3×3 supercell used in the calculations. The crosses indicate the in-plane positions used in obtaining the potential energy surface (PES). (b) Calculated PES for a Ag adatom on the H/Si(111) 1×1 surface whose area is indicated by the rectangle in (a). Sites H_3, T_4, and T_1 are (meta)stable binding sites, while S describes the saddle points. The energy contour spacing is 0.04 eV with respect to the most stable binding site H_3. The equivalent positions due to the symmetry of the H-terminated substrate without any Ag adatom are discriminated by superscripts.

In obtaining the PES, we first fix the Ag adatom at a site in the lateral direction with the initial heights of 2.5 Å from the surface hydrogen, and then relax all the surrounding atoms and also the adatom itself in the vertical direction. We repeat these calculations for 37 in-plane positions of the adatom in the two-dimensional uniform mesh spaced 0.74 Å apart [crosses in Fig. 1(a)] and then interpolate the calculated total energies (with respect to that of the lowest-energy site) with 37 plane waves to obtain global features of the PES.

In the PES, there are three (meta)stable binding sites at H_3, T_4, and T_1. The equilibrium atomic structures for these binding sites are displayed in Fig. 2. H_3 is the most stable binding site with the binding energy of 0.51 eV. In the H_3 structure, the Ag adatom is threefold coordinated with the top layer of Si atoms. All the three Si-Ag bonds have a bond length of 2.81 Å. The T_4 binding structure is the next stable structure with the binding energy less than the H_3 structure by 0.11 eV. In this structure, the Ag adatom makes an additional bond with the second layer Si atom with a 2.82 Å bond

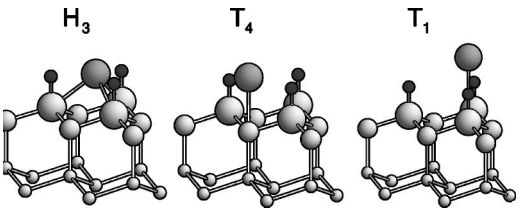

FIG. 2. Stable atomic structures for the Ag adatom adsorbed at sites H_3, T_4, and T_1 on H/Si(111) 1×1. White, black, and gray spheres represent Si, H, and Ag atoms, respectively.

length. In the T_1 site with the smallest binding energy of 0.24 eV, the Ag adatom is located just above the H atom bonded to the substrate. The bond length between the H atom and substrate Si atom is 1.58 Å, expanded slightly from that on H/Si(111), 1.50 Å, and bond length of the Ag-H is 1.94 Å.

The diffusion barrier for the Ag adatom diffusion on the surface and their pathway are easily obtained from the calculated PES (Fig. 1). The Ag adatom at the lowest-energy site H_3 slides to the next stable T_4 site passing through the nearby saddle point S without distinct substrate reconstruction. The required activation energy (E_a) is 0.14 eV for $H_3 \rightarrow T_4$ and 0.03 eV for the reverse process. This is in sharp contrast to the Si adatom on the H/Si(111) surface, where the calculated diffusion barrier is 1.3 eV.[20]

For a complete understanding of the diffusion process, we need to know the prefactor as well as the activation energy, since the diffusion rate at temperature T is expressed as $\Gamma = \Gamma^0 e^{-E_a/k_B T}$, where E_a is the energy barrier between two equilibrium sites for diffusion, and Γ^0 is the "attempt-to-diffuse" frequency prefactor, which can be obtained by the transition-state theory (TST) within the harmonic approximation.[21–24] The frequency prefactor is given by $\Gamma^0 = \Pi_{i=1}^{3N} \nu_i / \Pi_{i=1}^{3N-1} \nu_i^*$,[21] where ν_i (ν_i^*) are the normal-mode frequencies of the system with the Ag adatom at an equilibrium site (saddle points), and $3N$ is the number of degrees of freedom of the system. In principle, the adatom diffusion is a dynamical process affected by the entropic contribution of all the surrounding atoms in the $3N$-dimensional configuration space, which is dependent on details of the structure and the temperature. However, as mentioned earlier, the distortions of the substrate structure generated by adatom adsorption is nearly negligible, which implies that the dynamics of the substrate contribute only very little to the adatom diffusion process.[23,24] Thus we calculate normal-mode frequencies using the force-constant matrix derived from the obtained PES with the adiabatic approximation, which considers only the vibration frequencies of the adatom and static diffusion for zero temperature.[24] The frequency prefactors for $H_3 \rightarrow T_4 (\Gamma_1^0)$ and the reverse process (Γ_2^0) are calculated at 1.0×10^{11} and 6.7×10^9 s^{-1}, respectively,[27] implying $\Gamma_1 = 0.44 \times 10^9$ s^{-1} and $\Gamma_2 = 2.1 \times 10^9$ s^{-1} at room temperature.

Assuming only single jumps between the metastable sites,[28] we solve the master equation in the long-time limit within the random-walk model to obtain the isotropic tracer diffusion coefficient as $D = (\Gamma_1 \Gamma_2) a^2 / 2(\Gamma_1 + \Gamma_2)$,[25,26] where a is the lattice constant of the surface (3.86 Å). For the values of Γ_1 and Γ_2 at RT, the diffusion coefficient becomes 2.73×10^{-7} cm^2/s.

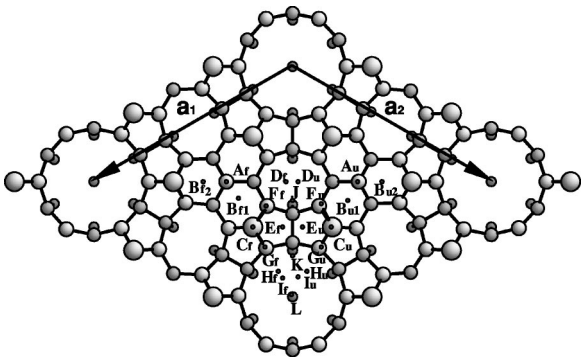

FIG. 3. In-plane positions (black dots) of the Ag adatom for the (meta)stable binding structures on the clean Si(111) 5×5 surface. The arrows designated by $\mathbf{a}_1$ and $\mathbf{a}_2$ are the surface lattice vectors of the Si(111) 5×5 unit cell. Subscripts f and u indicate adsorption inside FHUC and UHUC, respectively. Sites J and K are located on the boundary between two HUC's and site L on the corner hole Si atom.

B. Ag on the Si(111) Surface

It is well known that the clean Si(111) surface forms the 7×7-reconstructed structure, which consists of two different HUC's, a faulted-HUC (FHUC) and unfaulted-HUC (UHUC), separated by dimer rows.[29] Each HUC contains six Si adatoms and three Si rest atoms, which are locally arranged with 2×2 periodicity. According to the recent STM studies of the submonolayer metal atoms on the Si(111) 7×7 surface, the metal adatom diffusion is composed of two manifestly different processes: diffusion inside a HUC and out of a HUC.[13–16] The Si(111) 5×5 reconstructed structure[30] is a metastable structure with dimer rows, adatoms, rest atoms, and stacking faults, which are common in Si(111) 7×7. Thus the reduced Si(111) 5×5 surface is sufficient for obtaining the diffusion barrier between two HUC's. However, this surface has HUC's too small to study the diffusion within a HUC, since it contains only one Si rest atom in each HUC. For calculational efficiency, therefore, we use the Si(111) 5×5 surface for inter-HUC diffusion and the 4×4 supercell locally arranged with the 2×2 pattern for intra-HUC diffusion.

To obtain the diffusion barrier between two HUC's, we first explore the binding structures for the Ag adatom and find 12 (meta)stable binding sites in each HUC, labeled by *A–L* on Si(111) 5×5, where the equivalent positions of FHUC and UHUC are discriminated by subscripts f and u, respectively. Their in-plane binding sites and their relative energies are displayed in Fig. 3 and Table II, respectively. In our calculations, the Ag adatom is energetically more favorable in FHUC than in UHUC by 0.01–0.06 eV, like other metals Na (Ref. 15) and Pb (Ref. 14). The sites near the Si dangling bonds are relatively stable: for example, sites near the corner hole Si atom (*I* and *L*), Si rest atom (*A* and *B*), and Si adatom (*C*, *F*, and *G*). The most stable binding site is I_f near the corner hole Si on the FHUC side with a binding energy of 2.42 eV. The next lowest-energy site *B* bridges the Si rest atom and nearby adatom on the FHUC side. The Si rest-atom site *A* has a slightly higher energy than the *B* site

TABLE II. Relative energies (E) for the (meta)stable structures in FHUC. ΔE is the energy difference between adsorption structures in UHUC and FHUC, i.e., $E_{\mathrm{UHUC}}-E_{\mathrm{FHUC}}$. The values in the parentheses represent the Ag binding energies (E_b), i.e., $E_b=E_{\mathrm{Si}\ 5\times5}+E_{\mathrm{Ag}}-E_{\mathrm{Ag/Si}\ 5\times5}$, where $E_{\mathrm{Si}\ 5\times5}$, E_{Ag}, and $E_{\mathrm{Ag/Si}\ 5\times5}$ are the total energy of Si(111) 5×5 without a Ag adatom, the atomic energy of a Ag atom, and the total energy of Si(111) 5×5 with a Ag adatom, respectively.

Structure	E(eV)	ΔE(eV)
A	0.16 (2.22)	0.01
B	0.00 (2.38)	0.03
C	0.38 (2.00)	0.03
D	0.76 (1.62)	0.03
E	0.96 (1.42)	0.01
F	0.37 (2.01)	0.06
G	0.43 (1.95)	0.06
H	1.11 (1.27)	0.01
I	−0.04(2.42)	0.05
J	0.79 (1.59)	-
K	0.71 (1.67)	-
L	0.07 (2.31)	-

by 0.16 eV in FHUC. On the other hand, the binding sites near the boundary between two HUC's have relatively higher energies: for example, the D_f site between two dimers and the E_f site near a dimer axis have higher energies than the B_f site by 0.76 and 0.96 eV, respectively.

Instead of the PES approach that requires a lot of computational cost due to the large unit cell, we use the nudged elastic band method[31] for the diffusion processes of the Ag adatom. Diffusion of the adatom can be considered as a transformation of one (meta)stable state to another in the $3N$-dimensional configuration space, where N is the number of atoms in the unit cell. The resulting in-plane trace of the adatom corresponds to its diffusion pathway on the surface.

We consider diffusion process starting from the B site inside a HUC (the most stable site I is surrounded by energetically unfavorable sites, H and K, and a corner hole occupies a relatively small area, 7.4% for the 7×7 reconstruction). For the diffusion from one HUC to the next HUC, the Ag adatom can take three distinct pathways: passing through a dimer on the dimer row, between two dimers, or through a corner hole. For the diffusion crossing between two dimers, the most probable pathway follows B_{f2}, A_f, D_f, D_u, A_u, and B_{u2} with the overall activation energies $E_{f\rightarrow u}=0.88$ eV for FHUC$\rightarrow$UHUC and $E_{u\rightarrow f}=0.85$ eV for UHUC$\rightarrow$FHUC (Fig. 4). Since this activation energy is smaller than the energy difference between sites B and E, which is the minimum of the activation energy for pathways through E, the diffusion process passing above a dimer is unlikely. To calculate the diffusion barrier for crossing a corner hole, we consider two processes $B_{f1}\rightarrow C_f\rightarrow G_f\rightarrow K\rightarrow I_f$ and $B_{f1}\rightarrow C_f\rightarrow G_f\rightarrow I_f$ (see Fig. 5). In any case, the total activation energies are about 1.18 eV. Therefore, the diffusion process for passing the corner hole region is also energetically unfavorable. In brief, the Ag adatom migrate to an adjacent HUC passing between two dimers with the diffusion barrier of 0.88 eV (FHUC$\rightarrow$UHUC) or 0.85 eV (UHUC$\rightarrow$FHUC). Other possible diffusion processes are summarized in Table III.

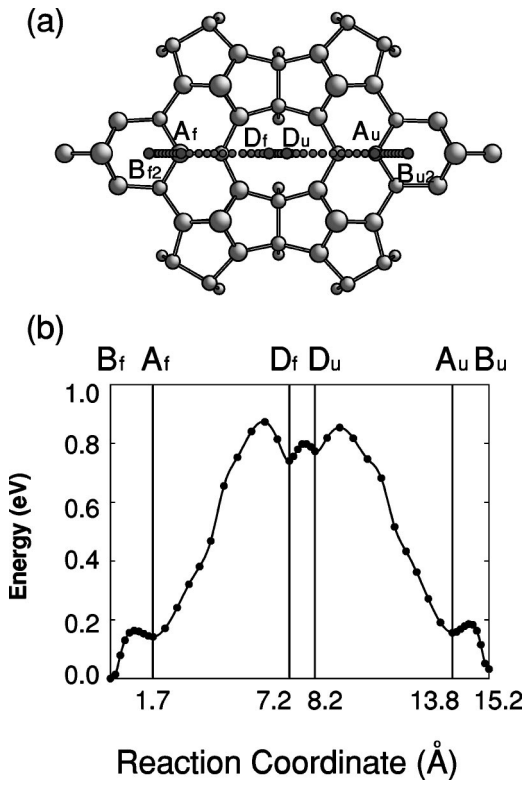

FIG. 4. (a) Top view of the diffusion pathway of the Ag adatom between two dimers, $B_{f2}\rightarrow B_{u2}$. The adatom passes through sites A_f, D_f, D_u, and A_u. The larger dots indicate the (meta)stable adsorption sites. (b) The corresponding energy variation along the pathway in (a).

In order to obtain the diffusion barrier of a Ag atom inside a HUC, we have performed another calculation on the Si(111) 2×2 (of the 4×4 supercell), which corresponds to the local periodicity of a UHUC.[32] The metastable binding sites and their relative energies are displayed in Fig. 6 and Table IV, respectively. The most stable site is B_2, which bridges two Si atoms with dangling bonds, i.e., the adatom and nearby rest atom. It is of note that the site just above the rest atom T_1 is the next stable site. The present results are rather different from the behaviors of metal adsorbates with other valences (K, Mg, and Ga).[33] It was calculated that the most stable binding site, as in the present case, is B_2 and that the favorable binding sites (T_4 and B_2) assembled around the unstable rest-atom site form an "attractive basin."[33] However, for Ag case, T_1 is more stable than the nearby highly coordinated T_4 site, which implies that the basin (the belt of stable sites) does not form in this case.

From investigation of various possibilities, we determine the most probable diffusion pathway of a Ag adatom as shown in Fig. 6(a): $B_2^1\rightarrow T_1^1\rightarrow B_2^2\rightarrow T_1'^5\rightarrow B_2^4$ or $B_2^1\rightarrow T_1^1\rightarrow B_2^3\rightarrow T_1'^6\rightarrow B_2^5$. Two key processes, $B_2\rightarrow T_1$ and $B_2\rightarrow T_1'$, among the diffusion processes are displayed in Fig. 6(b). The rate-determining step is $B_2\rightarrow T_1'$ with the activation energy 0.27 eV, which becomes the diffusion barrier of the Ag ada-

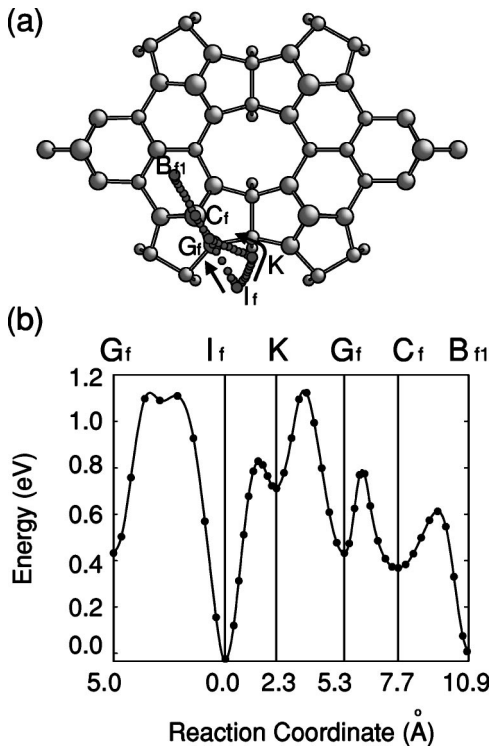

FIG. 5. (a) Top view of the diffusion pathway of the Ag adatom for the $I_f \rightarrow B_{f1}$ process, through the G_f site. Ag may migrate to G_f directly or via K. The arrows indicate these two pathways and the larger dots indicate the (meta)stable binding sites. (b) The corresponding energy variation along the pathway in (a).

tom on the Si(111) 2×2 surface or within a HUC of the Si(111) 7×7 surface. This magnitude of the diffusion barrier, though larger than that on the H/Si(111) 1×1 (0.14 eV), is still small. This can be interpreted by the fact that a relatively strong Ag-Si bond is preserved all along the diffusion paths.

Comparing the 2×2 and 5×5 surfaces, the T_1, T_1', and B_2 sites on the diffusion paths of the Ag adatom on the 2×2 surface correspond to the A_u, F_u, and B_u sites on the 5×5 surface, respectively (refer to Figs. 3 and 6). The binding energy differences are 0.07, 0.09, and 0.06 eV for $T_1(A_u)$, $T_1'(F_u)$, and $B_2(B_u)$ sites, respectively (Tables II and IV). Although the differences are not negligible compared with the diffusion barrier 0.27 eV on the Si(111) 2×2, they will give only a marginal effect to our conclusions since a diffusion barrier is related not with the energy itself but with the energy difference (between the metastable and saddle-point structures). Indeed, we can see the diffusion barrier (0.18 eV) of the $B_2 \rightarrow T_1$ process on the 2×2 surface coincides with that of the equivalent process of $B_u \rightarrow A_u$ on the 5×5 surface. Thus our diffusion barriers obtained using the different surfaces (2×2 and 5×5) appear consistent and reliable for describing Ag behaviors on the clean Si(111) surface.

TABLE III. Diffusion barrier (E_a) and corresponding energy change (ΔE) for each diffusion process.

Process	E_a(eV)	ΔE(eV)
$B_f \rightarrow A_f$	0.18	0.16
$B_f \rightarrow C_f$	0.61	0.38
$B_f \rightarrow F_f$	0.40	0.37
$A_f \rightarrow D_f$	0.73	0.60
$F_f \rightarrow J$	0.64	0.42
$F_f \rightarrow D_f$	0.70	0.39
$D_f \rightarrow D_u$	0.06	0.03
$A_u \rightarrow D_u$	0.68	0.62
$B_u \rightarrow A_u$	0.19	0.17
$I_f \rightarrow K$	0.86	0.75
$I_f \rightarrow G_f$	1.18	0.47
$G_f \rightarrow C_f$	0.34	−0.05
$K \rightarrow G_f$	0.41	−0.28

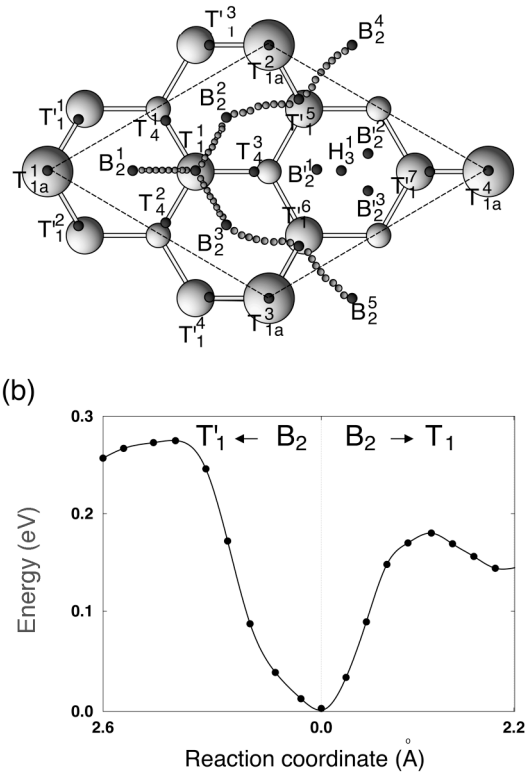

FIG. 6. (a) Top view of the in-plane positions of (meta)stable binding sites (black dots) and the diffusion pathway (gray dots) for the Ag adatom on the Si(111) 2×2 surface (dashed lines). The equivalent positions due to surface symmetry are discriminated by superscripts. The Ag adatom at the lowest-energy site B_2 migrates to the neighboring equivalent sites, along the pathway ($B_2^1 \rightarrow T_1^1 \rightarrow B_2^2 \rightarrow T_1'^5 \rightarrow B_2^4$ or $B_2^1 \rightarrow T_1^1 \rightarrow B_2^3 \rightarrow T_1'^6 \rightarrow B_2^5$). (b) The energy variations for two key processes in (a): $B_2 \rightarrow T_1$ and $B_2 \rightarrow T_1'$.

For the clean surface, we do not calculate the frequency prefactors since a large computational cost is required due to the large unit cell of the clean surface and hence due to complex diffusion process. Instead, we adopt values determined in the recent STM experiment of Sobotik *et al.*:[16] $8\times10^{(10\pm1)}$ and $2\times10^{(10\pm0.8)}$ s^{-1} at FHUC and UHUC, respectively. The frequency prefactors are averaged all over the HUC since they are obtained by assuming that a whole HUC with a large area contains a single binding site. The measured

TABLE IV. Relative energies (E) for the (meta)stable adsorption sites of a Ag adatom on faulted and unfaulted Si(111) 2×2 [refer to Fig. 6(a)], which are discriminated by subscripts f and u, respectively. The values in the parentheses represent the Ag binding energies (E_b), i.e., $E_b=E_{\mathrm{Si}\ 2\times2}+E_{\mathrm{Ag}}-E_{\mathrm{Ag/Si}\ 2\times2}$, where $E_{\mathrm{Si}\ 2\times2}$, E_{Ag}, and $E_{\mathrm{Ag/Si}\ 2\times2}$ are the total energy of Si(111) 2×2 without a Ag adatom, the atomic energy of a Ag atom, and the total energy of Si(111) 2×2 with a Ag adatom, respectively. The T_{1a} site indicates the on-top site of a Si adatom and the others denote the usual positions without Si adatom. Note that the 4×4 supercell is used in all calculations.

Structure	T_{1a}	T_1	T_4	B_2	T_1'	H_3	B_2'
E_f(eV)	0.68 (1.64)	0.15 (2.17)	0.39 (1.93)	0.00 (2.32)	0.25 (2.07)	0.69 (1.63)	0.77 (1.55)
E_u(eV)	0.70 (1.59)	0.15 (2.14)	0.38 (1.91)	0.00 (2.29)	0.25 (2.04)	0.69 (1.60)	0.79 (1.50)

frequency prefactors and the calculated diffusion barriers give the hopping rates at RT of 4.1×10^{-5} and 3.4×10^{-5} s^{-1} out of FHUC and UHUC, respectively. In contrast, the diffusion rate within a HUC is larger than those between HUC's by $\sim10^{10}$ at RT assuming the same frequency prefactors. It is clear that the diffusion rates between the HUC's are extremely low compared to those for the hydrogenated Si(111) surface or for the Si(111) 2×2 surface (i.e., within a HUC); hence formation of large Ag islands will be effectively suppressed on the clean surface with dimer-row boundaries.

IV. DISCUSSION

On the H-terminated Si(111) surface, all the stable structures as well as the saddle-point structures for Ag adsorption have small binding energies less than 0.51 eV, because all the Si dangling bonds are saturated by H atoms. These small magnitudes and variations in the binding energy give rise to the extremely small diffusion barrier of 0.14 eV. The calculated diffusion rate for hopping out of the one unit cell is $\sim10^9$ s^{-1} at RT. Thus, a Ag atom, once adsorbed on the H/Si(111) surface, has a high probability to encounter other Ag atoms or islands and tends to aggregate into bigger islands. To discuss the growth mode of thin Ag films on H/Si(111), we need one more variable, the Schwoebel barrier, which an adatom encounters in crossing the step edge from the upper area of an island to the substrate.[34] The Schwoebel barrier, although to be confirmed, is expected to be large because of the small binding energy on the hydrogenated surface and the large Ag-Ag interaction energy.[35] This means that a Ag adatom adsorbed on a Ag island tends to continue to stay on the island with strong Ag-Ag binding energies rather than to go down to the substrate with small binding energy. In this way, three-dimensional islands would be formed. This expectation is consistent with experimental observation for Ag growth on the H/Si(111) surface, i.e., the VW mode.[2,9–11]

The diffusion barrier 0.27 eV for Ag migration inside a HUC on Si(111) 7×7, despite the presence of dangling bonds implying large binding energies, differs little from that for Ag on the H/Si(111) surface. Looking into the diffusion pathways in Fig. 6, the Ag atom always makes bonds with the substrate Si atoms (with a dangling bond) all along the pathways. This implies small energy variations along the paths and hence small diffusion barriers. On the other hand, the energy barriers for inter-HUC diffusion increase significantly: 0.88 eV for the hopping from a FHUC to an UHUC and 0.85 eV for the reverse. These values agree quite well with the measurement by Sobotik *et al.*, 0.93 ± 0.07 and 0.81 ± 0.05 eV for two inter-HUC processes.[16] The increase in the barriers for inter-HUC diffusion can be understood from the difference in chemical environment between the areas inside HUC's and near the boundaries. Unlike the area within a HUC, the dimer rows between two HUC's have no dangling bond that can make strong bonds with the Ag adatom. Thus the adatom near the dimer rows has higher energy than within the HUC (refer to Table II). Indeed, this argument is seen in Fig. 4 where the rate-determining steps occur when the Ag adatom diffuses near the boundary of HUC's, such as $A_f\rightarrow D_f$ and $A_u\rightarrow D_u$.

The contrast of the diffusion barriers (the smaller for intrahopping and the larger inter-HUC hopping) provides a useful understanding of the initial-stage Ag growth on the Si(111) 7×7 surface. The Ag clusters with small sizes would be easily formed inside HUC's at submonolayer coverages.[13] Furthermore, the large diffusion barrier for inter-HUC hopping, e.g., the low diffusion rate of 10^{-5} s^{-1} at RT, would suppress Ag-island formation and, as a result, play an important role in formation of a wetting layer.[13] After that, further Ag deposition could result in formation of three-dimensional (with $\sqrt{3}\times\sqrt{3}$ phase transition) or two-dimensional islands depending on the substrate temperature.

Finally, we briefly mention the role of the corner hole dangling bond, which becomes a stable binding site for the Ag adatom. However, the energy barriers from the corner hole to the nearest HUC and for the reverse process is very high (1.18 and 1.14 eV, respectively). In addition, since a corner hole occupies a small area [$\sim$7.4% on Si(111) 7×7], the amount of Ag adatoms adsorbed onto the corner holes would be small and would not affect significantly the Ag growth mode.

V. CONCLUSION

In conclusion, we have investigated the adsorption and diffusion of a Ag adatom on both the H-terminated and clean Si(111) surfaces, using first-principles pseudopotential calculations. On the H/Si(111) surface, the Ag adatom almost freely moves with an extremely small diffusion barrier of 0.14 eV. For Ag on the clean Si(111) surface, on the other hand, we have found two major processes for moving inside a HUC and between two HUC's with barriers of 0.27 and 0.88 eV, respectively. This difference results from the differ-

ent chemical environments: the inside of the HUC with dangling bonds versus the boundaries between HUC's without any dangling bond. The large barrier for inter-HUC diffusion would suppress three-dimensional island formation on the Si(111) 7×7 surface and would be helpful in forming a wetting layer. The present results provide a theoretical framework for understanding Ag growth behaviors on both kinds of surfaces.

ACKNOWLEDGMENTS

The authors would like to acknowledge support from KISTI (Korea Institute of Science and Technology Information) under "the 5th Strategic Supercomputing Applications Support Program" with Dr. Sang-Min Lee as the technical supporter. The use of the computing system of the Supercomputing Center is also greatly appreciated.

*Email address: jsm@chonbuk.ac.kr

[1] M. Copel, M. C. Reuter, E. Kaxiras, and R. M. Tromp, Phys. Rev. Lett. **63**, 632 (1989).
[2] K. Sumitomo, T. Kobayashi, F. Shoji, K. Oura, and I. Katayama, Phys. Rev. Lett. **66**, 1193 (1991).
[3] S. Jeong and A. Oshiyama, Phys. Rev. Lett. **79**, 4425 (1997) and references therein.
[4] K. Oura, V. G. Lifshits, A. A. Saranin, A. V. Zotov, and M. Katayama, Surf. Sci. Rep. **35**, 1 (1999).
[5] H. Hirayama, H. Okamoto, and K. Takayanagi, Phys. Rev. B **60**, 14 260 (1999).
[6] S. Tosch and H. Neddermeyer, Phys. Rev. Lett. **61**, 349 (1988).
[7] L. Huang, S. J. Chey, and J. H. Weaver, Surf. Sci. **416**, L1101 (1998).
[8] L. Gavioli, K. R. Kimberlin, M. C. Tringides, J. F. Wendelken, and Z. Zhang, Phys. Rev. Lett. **82**, 129 (1999).
[9] J. M. Zuo and B. Q. Li, Phys. Rev. Lett. **88**, 255502 (2002); Surf. Sci. **520**, 7 (2002).
[10] A. Nishiyama, G. ter Horst, P. M. Zagwijn, G. N. van den Hoven, J. W. M. Frenken, F. Garten, A. R. Schlatmann, and J. Vrijmoeth, Surf. Sci. **350**, 229 (1996).
[11] Y. Ohba, I. Katayama, Y. Yamamoto, and M. Watamori, Appl. Surf. Sci. **113-114**, 448 (1997).
[12] N. Enomoto, T. Hoshino, M. Hata, and M. Tsuda, Appl. Surf. Sci. **130-132**, 237 (1998).
[13] J. Myslivecek, P. Sobotik, I. Ostadal, T. Jarolimek, and P. Smilauer, Phys. Rev. B **63**, 045403 (2001); P. Sobotik, I. Ostadal, and P. Kocan, Surf. Sci. **507-510**, 389 (2002); T. Jarolimek, J. Myslivecek, P. Sobotik, and I. Ostadal, *ibid.* **482-485**, 386 (2001); P. Sobotik, I. Ostadal, J. Myslivecek, and T. Jarolimek, *ibid.* **482-485**, 797 (2001).
[14] J. M. Gomez-Rodriguez, J. J. Saenz, A. M. Baro, J. Y. Veuillen, and R. C. Cinti, Phys. Rev. Lett. **76**, 799 (1996); P. Jelinek, M. Ondrejcek, J. Slezak, and V. Chab, Surf. Sci. **544**, 339 (2003).
[15] K. Wu, Y. Fujikawa, T. Nagao, Y. Hasegawa, K. S. Nakayama, Q. K. Xue, E. G. Wang, T. Briere, V. Kumar, Y. Kawazoe, S. B. Zhang, and T. Sakurai, Phys. Rev. Lett. **91**, 126101 (2003).
[16] P. Sobotik, P. Kocan, and I. Ostadal, Surf. Sci. **537**, L442 (2003).
[17] G. Kresse and J. Hafner, Phys. Rev. B **47**, R558 (1993); G. Kresse and J. Furthmuller, *ibid.* **54**, 11169 (1996).
[18] D. Vanderbilt, Phys. Rev. B **41**, R7892 (1990).
[19] J. P. Perdew, in *Electronic Structure of Solids '91*, edited by P. Ziesche and H. Eschrig (Academie Verlag, Berlin, 1991).
[20] S. Jeong, Surf. Sci. **530**, 155 (2003).
[21] G. H. Vineyard, J. Phys. Chem. Solids **3**, 121 (1957).
[22] T. Ala-Nissila, R. Ferrando, and S. C. Ying, Adv. Phys. **51**, 949 (2002).
[23] C. Ratsch and M. Scheffler, Phys. Rev. B **58**, 13 163 (1998).
[24] G. Boisvert and L. J. Lewis, Phys. Rev. B **54**, 2880 (1996).
[25] A. Natori and R. W. Godby, Phys. Rev. B **47**, 15 816 (1993).
[26] E. Penev, S. Stojkovic, P. Kratzer, and M. Scheffler, Phys. Rev. B **69**, 115335 (2004).
[27] The compensation effect is seen here: A lower attempt frequency for a lower diffusion barrier [W. Meyer and H. Nedal, Z. Tech. Phys. (Leipzig) **12**, 588 (1937)].
[28] The double-jump process for $H_3\rightarrow H_3$ would be possible due to the extremely small diffusion barrier of 0.03 eV for $T_4\rightarrow H_3$. In this case, the diffusion coefficient for adatom diffusion is changed to $D=[(3-2\alpha)\Gamma_1\Gamma_2]a^2/2(\alpha\Gamma_1+\Gamma_2)$, where α is the equilibration probability in the T_4 site which varies between 0 (complete double jumps) and 1 (single jumps only), and the rates for $H_3\rightarrow T_4$ and $H_3\rightarrow H_3$ are assumed to be $\alpha\Gamma_1$ and $(1-\alpha)\Gamma_1$, respectively (Ref. 26). At RT, the upper limit of diffusion coefficient for $\alpha=0$ is 9.94×10^{-7} cm^2/s, which is only larger 3.6 times than the lower limit for $\alpha=1$.
[29] K. Takayanagi, Y. Tanishiro, S. Takahashi, and M. Takahashi, J. Vac. Sci. Technol. A **3**, 1502 (1985).
[30] R. S. Becker, J. A. Golovchenko, G. S. Higashi, and B. S. Swartzentruber, Phys. Rev. Lett. **57**, 1020 (1986).
[31] G. Mills, H. Jonsson, and G. K. Schenter, Surf. Sci. **324**, 305 (1995).
[32] The adsorption geometries and their energetics for the Ag adatom on the faulted Si(111) 2×2 surface corresponding to the local structure in FHUC are almost the same as those on unfaulted Si(111) 2×2 surface (see Table IV), which implies that the diffusion processes of the Ag adatom are nearly identical on both surfaces.
[33] K. Cho and E. Kaxiras, Surf. Sci. **396**, L261 (1998).
[34] R. L. Schwoebel and E. J. Shipsey, J. Appl. Phys. **37**, 3682 (1966).
[35] The cohesive energy per atom of bulk Ag and the binding energy per atom of two-atom Ag cluster are calculated at 2.31 and 1.08 eV, respectively, which are much larger than the Ag binding energy on the H/Si(111) surface.
[36] C. Kittle, *Introduction to Solid State Physics*, 7th ed. (Wiley, New York, 1996).
[37] D. R. Lide and H. P. R. Frederikse, *Handbook of Chemistry and Physics*, 78th ed. (CRC Press, Boca Raton, 1997).